International Journal of Fatigue 174 (2023) 107711

Contents lists available at ScienceDirect

International Journal of Fatigue

journal homepage: www.elsevier.com/locate/ijfatigue

Fatigue Behaviour of Additively Manufactured Short Fibre Reinforced Polyamide

A. Panerai [a], A. Canegrati [a], L.M. Martulli [a,*], M. Kostovic [b], G. Rollo [b], A. Sorrentino [b], M. Carboni [a], A. Bernasconi [a]

[a] Politecnico di Milano, Department of Mechanical Engineering, Via La Masa 1, 20156 Milano, Italy
[b] Polymer, Composites and Biomaterials Institute, National Research Council (CNR), Via Previati 1/E, 23900 Lecco (LC), Italy

ARTICLE INFO

Keywords:
Carbon Fibre
Discontinuous Reinforcement
Polymer-matrix Composites
Mechanical Testing
Additive Manufacturing

ABSTRACT

Additive manufacturing of Short Fibre Reinforced Polymers (SFRPs) combines good mechanical properties with high design flexibility. In this work, fatigue tests were performed on SFRP specimens with 0°/90° and ±45° raster orientations. Thermal and mechanical fatigue regimes were both observed. In thermal fatigue, self-heating, softening and changes in viscoelastic properties occurred. In mechanical fatigue, the material progressively stiffened, and dissipative effects due to viscoelasticity were reduced. Such a behaviour is unusual for composites, but mainly seen in neat polymers. These results suggest the fatigue behaviour of this material to be dominated by the polyamide matrix.

1. Introduction

Additive Manufacturing (AM) is gaining increasing importance in various industrial fields, thanks to its design flexibility and ability to create complex geometries at relatively low cost. Fused Filament Fabrication (FFF) is one of the most popular AM technologies available for polymers [1]. FFF is an AM technology in which a thermoplastic filament is heated and extruded through a nozzle and deposited in a specific path to form a planar layer of the final object [1], which is thus manufactured layer-by-layer [2]. Thermoplastic parts printed through FFF are usually not strong enough to be used in engineering applications as fully functional and load-bearing components [3]. The use of Short Fibre Reinforced Polymers (SFRPs) as printing materials can overcome this limitation by improving parts' strength and stiffness [4].

FFF-printed parts are characterized by a strong anisotropy, as the mechanical properties along the printed bead are higher than across it [5,6]. Printing pattern and building orientation therefore play a major role in the mechanical properties of a finished part. In the case of FFF printing of SFRPs, anisotropy is even higher, because during printing the flow of extruded material causes fibres in the printed bead to align mainly with the printing direction [7]. Strength and stiffness of the bead along the printing direction are thus significantly increased [8–10], while inter-bead strength is barely affected [9].

Several studies have explored the static properties of FFF printed SFRPs [3,4,6–11]. The fatigue behaviour is instead less known, and its analysis is more complex [5]. It may depend on the fatigue behaviour and strength of the matrix, fibres, and matrix-fibre interface, on printing parameters, or on the strength of the bonds between each printed bead and between layers. Considering the current scarcity of works on the fatigue properties of FFF printed SFRPs, it is worth reviewing the fatigue behaviour of similar materials, namely neat polymers, SFRPs, and FFF printed materials.

The fatigue analysis of polymers requires the knowledge of the viscoelastic properties involved in the fatigue damage processes. Fig. 1 shows an example of the stress–strain response of a viscoelastic material to a cyclic load with positive load ratio (both minimum and maximum applied loads are positive). Some important parameters to understand material behaviour are here explained for clarity. Because of viscoelasticity, some energy is dissipated as heat under cyclic loading, causing the specimen temperature to increase. The amount of dissipated energy is related to the hysteresis area (highlighted in grey in Fig. 1). The dynamic modulus E_{Dyn} represents the stiffness of the material, and is related to the slope of the hysteresis cycle (i.e., of the dashed line in Fig. 1). This indication of stiffness represents the instantaneous response of the material, and is not affected by creep [12].

During fatigue testing of polymers, hysteretic heating causes a significant increase in the temperature of the specimens, even at low frequencies [12]. This increase in temperature influences the material

* Corresponding author.
E-mail address: lucamichele.martulli@polimi.it (L.M. Martulli).

https://doi.org/10.1016/j.ijfatigue.2023.107711
Received 10 February 2023; Received in revised form 17 April 2023; Accepted 7 May 2023
Available online 15 May 2023

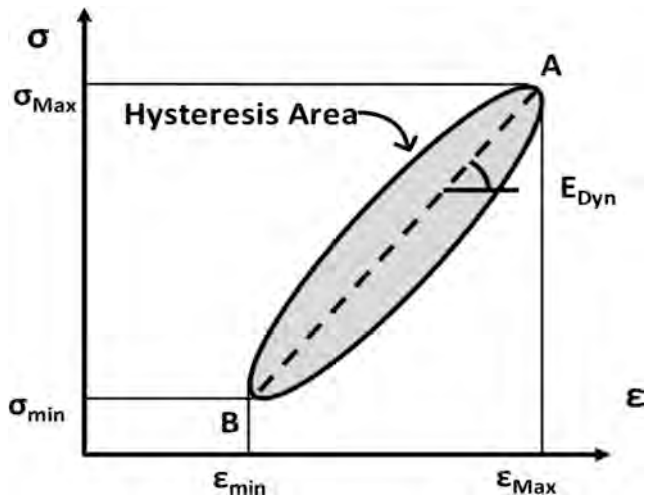

Fig. 1. Schematic representation of the stress–strain response of a polymeric material to a cyclic load.

response during fatigue loading, as polymers are quite sensitive to temperature changes, especially when they are tested close to their glass transition temperature (T_G) [8]. As an example, the T_G of Polyamide, which is the matrix material of the composite investigated in this work, ranges between 60 and 80 °C in dry conditions, but it drops to around room temperature after the material has been exposed to a humid environment [13]. This makes the material less stiff and more ductile [13]. In parts produced by FFF, this effect is quite critical: due to the manufacturing-induced porosity of the material, water diffusion inside the material is very fast [6].

Fatigue of injection moulded polymer is characterized by two regimes, known as the thermal fatigue regime, and the mechanical fatigue regime [12,14–18]. The thermal fatigue regime occurs in the first stage of a fatigue test, when hysteretic heating causes a continuous increase in the specimen's temperature. Specimens tested under high level applied loads and high testing frequencies fail in this regime, and experience during their fatigue life a continuous decrease in modulus and increase in dissipation due to thermal softening [14]. For lower applied loads, the polymer does not heat up indefinitely, but an equilibrium temperature is reached [17]. When temperature has stabilized, mechanical fatigue takes place, and failure occurs due to crack initiation and propagation [1217]. In this regime, even though the temperature has increased, the polymer becomes stiffer [14,16–19] as fatigue progresses, and its dissipation decreases [14,16,17,20], which can actually cause the specimen temperature to slightly decrease over time [12,16,20].

In fatigue of injection moulded SFRPs, thermal and mechanical fatigue regimes are also present. Esmaeillou et al. [21] observed that for higher applied fatigue loads the specimen temperature continuously increased until failure due to matrix self-heating, while for lower applied loads it eventually stabilized and remained virtually constant until shortly before failure. However, the mechanical behaviour of SFRPs during fatigue is different than that of neat injection moulded polymers, as their stiffness decreases in mechanical fatigue [21–23]. Indeed, in [23] both SFRP and matrix-only specimens were tested under tensile-tensile fatigue in the mechanical fatigue regime; the stiffness of the SFRP specimens decreased, while that of the matrix-only specimens increased. This difference is due to the different damage mechanisms occurring in the composite, such as fibre breakage and debonding [23], which play the paramount role in determining the specimen's stiffness [23,24]. Interestingly, Noda et al. [25] observed for a polyamide-based SFRP a decrease in dissipation with fatigue, similarly to what observed in neat injection moulded polymers.

For what concerns FFF-printed materials, their fatigue behaviour is mainly affected by the raster orientation and the sequence of the layers, and the presence of printing defects [1]. Both tensile and fatigue strength are significantly lower than injection moulded specimens made of the same material [2,26,27]. While the UTS is usually higher for the 0° raster orientation [5,27], it was found that the ± 45° raster orientation shows a significantly higher fatigue strength [27]. To the authors' knowledge there are currently no works investigating the evolution of mechanical properties of FFF-printed materials under tensile fatigue. Terekhina et al. [28] investigated the flexural fatigue behaviour of FFF-printed Polyamide-6, and found that the stiffness decreased as fatigue progressed. This decrease was attributed to the growth of damage between printed beads [28]. They also observed a decrease in hysteresis area with fatigue, similarly to what observed in neat injection moulded polymers.

Several studies focus on the fatigue behaviour of neat polymer FFF-printed neat polymers, while the fatigue behaviour of SFRPs remains mainly unexplored. It is also not known how their mechanical properties may vary with fatigue. A variety of different factors may influence material behaviour, and it is currently not known how all of these factors may be contributing to the fatigue behaviour of SFRPs produced by FFF. In this study, SFRP specimens were printed by FFF and tested both statically and under tensile-tensile fatigue. To analyse the effect of raster orientation, specimens with 0°/90° and ±45° raster orientations were used. Static tensile tests were performed to determine the loads to be used in the fatigue tests. During fatigue testing, changes in mechanical properties as well as surface temperature were recorded to understand how fatigue influences the response of the material.

2. Materials and methods

2.1. Specimens manufacturing

The specimens tested in this work were printed using a MarkForged Onyx Pro FFF 3D printer. The material used is a polyamide-6,6 reinforced with short carbon fibres (approximately 16 % by weight [8]), developed by Markforged and sold under the trade name of Onyx [30]. The Markforged proprietary slicing software Eiger [31] prevents the user from printing unidirectional specimens (i.e., with all layers having the same raster orientation). Therefore, in this work, rectangular specimens were printed with two different alternating raster orientations, namely 0°/90° and ±45°, shown in Fig. 2. The specimens' nominal dimensions were 140 × 30 × 3.2 mm for 0°/90° specimens and 175 × 30 × 3.2 mm for ±45° specimens. The 0°-direction is the direction in which the load is applied during testing. Eiger software also imposes printing of two concentric contour rings to improve surface finish (see Fig. 2) [31]. End tabs (40 × 30 × 2 mm for 0°/90° specimens and 50 × 30 × 2 mm tabs for ±45° specimens) were also printed using Onyx, and then adhesively bonded onto the specimens using two-part epoxy to limit stress concentrations in the clamped portion [32]. The specimens can be seen in Fig. 3.

Before testing, all specimens were conditioned by keeping them in a controlled (23 °C, RH50%) environment, and weighing them regularly until no significant weight change was detected.

2.2. Tensile and fatigue tests

Quasi-static tensile tests were performed in displacement control according to ASTM D3039 on three 0°/90° and three ± 45° specimens using an electro-mechanical MTS Alliance RT/100 machine with a 100 kN load cell at a constant rate of 5 mm/min. An extensometer with a 50 mm gauge length was used to measure strain.

Load controlled tensile-tensile (R = 0.1) fatigue tests were performed according to ASTM D3479 using a servo-hydraulic MTS Landmark testing machine with a 100 kN load cell. A frequency of 2 Hz was used throughout. Applied stress ranges were 75%-90% of UTS for the 0°/90° specimens, and 45%-95% of UTS for ±45° specimens. Specimens that did not fail within one million cycles were considered runouts. The test

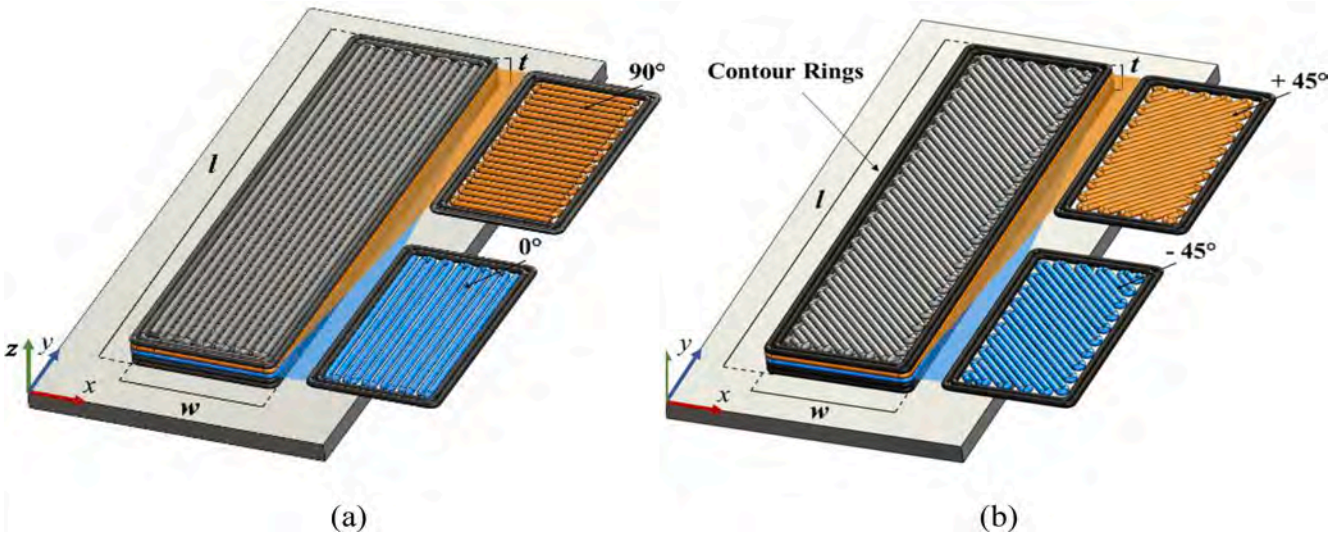

Fig. 2. Printing layout of the specimens showing the alternating raster pattern (in blue and orange) and the contour rings (grey) for the (a) 0°/90° and (b) ± 45° specimens. (For interpretation of the references to colour in this figure legend, the reader is referred to the web version of this article.)

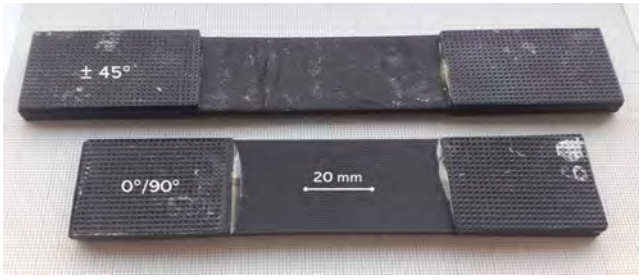

Fig. 3. 0°/90° and ± 45° specimens.

setup, shown in Fig. 4, included a resistance thermometer attached to a clip, which was used to measure surface temperature variations, and a hygrometer to measure environmental temperature and humidity, while force and displacements were measured by the machine itself. This test setup was chosen based on a previous work [33].

Fatigue tests were performed in a controlled environment (23 °C, 50% RH). Environmental measurements taken with the hygrometer showed that environmental fluctuations were kept within ±0.5 °C and ±1% RH during all the performed tests. A total of 24 fatigue tests were performed, 13 for 0°/90° and 11 for ±45° specimens.

During testing, the machine was set to record the stress and strain during the first 100 cycles, one every 10 cycles from 10^2 to 10^3 cycles, one every 100 cycles from 10^3 to 10^4 cycles, one every 1000 cycles from 10^4 to 10^5 cycles, and one every 10,000 cycles from 10^5 to 10^6 cycles, with a sample rate of 200 Hz. The strain was determined from the machine's crosshead displacement, which was shown to provide suitable accuracy in a previous investigation [33].

Fig. 4. Setup for fatigue testing.

3. Results

In Fig. 5 the tensile stress–strain plots are shown, while the results are summarized in Table 1. The Ultimate Tensile Strength (UTS) of the two raster orientations is rather similar, but their mechanical behaviour is significantly different, with ±45° specimens showing a strain at break about six times higher than 0°/90° ones, and a 60% lower elastic modulus. Onyx's mechanical behaviour is markedly nonlinear, as evidenced by the continually decreasing slope of the stress–strain plot, caused by stress relaxation during testing. A deeper analysis of the static behaviour can be found in Canegrati et al. [6].

The SN results of fatigue tests on 0°/90° and ±45° specimens are shown in Fig. 6. The SN curve of 0°/90° specimens shows, as expected, an increase in fatigue life with a decrease in the applied load, although there is a significant standard deviation. At one load (84% of UTS) failure occurred over several orders of magnitudes. For the ±45° raster orientation the results are more erratic, and either very rapid failure occurred or the test ended in a runout.

In Fig. 7, Fig. 8, Fig. 9, and Fig. 10 are shown the evolution of

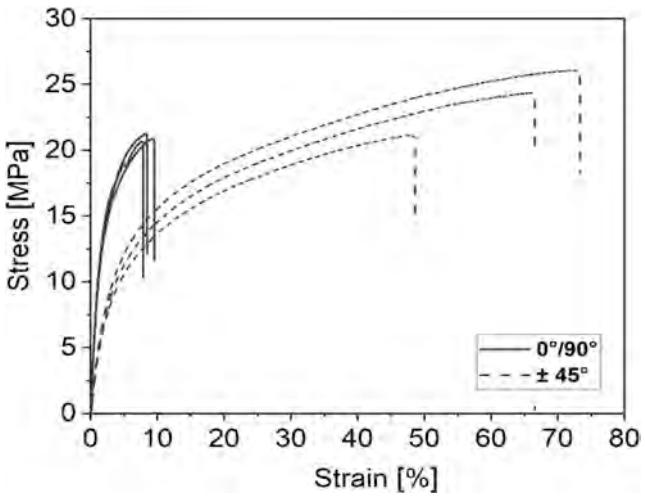

Fig. 5. Stress–strain plots of the tensile tests.

Table 1
Results of the tensile tests. '±' indicates standard deviation.

Orientation	Young's Modulus [MPa]	UTS [Mpa]	Strain at Break [%]
0°/90°	1074 ± 44.69	20.91 ± 0.307	10.5 ± 0.8
± 45°	412 ± 11.09	23.85 ± 2.50	62.7 ± 12.8

dynamic modulus, temperature, hysteresis area, and strain, respectively. The dynamic modulus was obtained by:

$$E_{Dyn} = \frac{\sigma_{Max} - \sigma_{min}}{\epsilon_{Max} - \epsilon_{min}}, \quad (1)$$

while the hysteresis loop area for each recorded cycle was obtained by numerical integration. Two ±45° specimens experienced failure very close to the tabs. Their failure was considered invalid, so they were not included in the SN curve, however they are included in the following graphs, as their mechanical behaviour up to failure was in line with the others.

It is possible to observe, for both raster orientations, that two distinct behaviours are present, one for high level loads and one for low level ones. At higher applied loads, the temperature increases throughout the test (Fig. 8), while the dynamic modulus decreases (Fig. 7). Failure occurs within the first few hundred cycles. At lower applied loads, specimens initially do show a softening trend (Fig. 7). However, after several fatigue cycles, the dynamic modulus increases, while the hysteresis area decreases (Fig. 9).

Hysteretic heating is significant, especially for ±45° specimens, where the increment of temperature is in the order of 10–20 °C (Fig. 8. b). Interestingly, after the initial heating period, temperature does not stabilize, but decreases over time (Fig. 8.a and 7.b). It can be observed that the specimens' temperature shows some periodic oscillations. These were caused by slight variations in environmental temperature caused by the conditioning system turning on and off. These oscillations appeared to visibly affect both temperature and modulus: each time temperature increased a slight increase in hysteresis area and decrease in dynamic modulus could be recorded (see Fig. 11). Nevertheless, their amplitude was small (< ±1 °C), and they did not appear to have an effect on the overall fatigue behaviour.

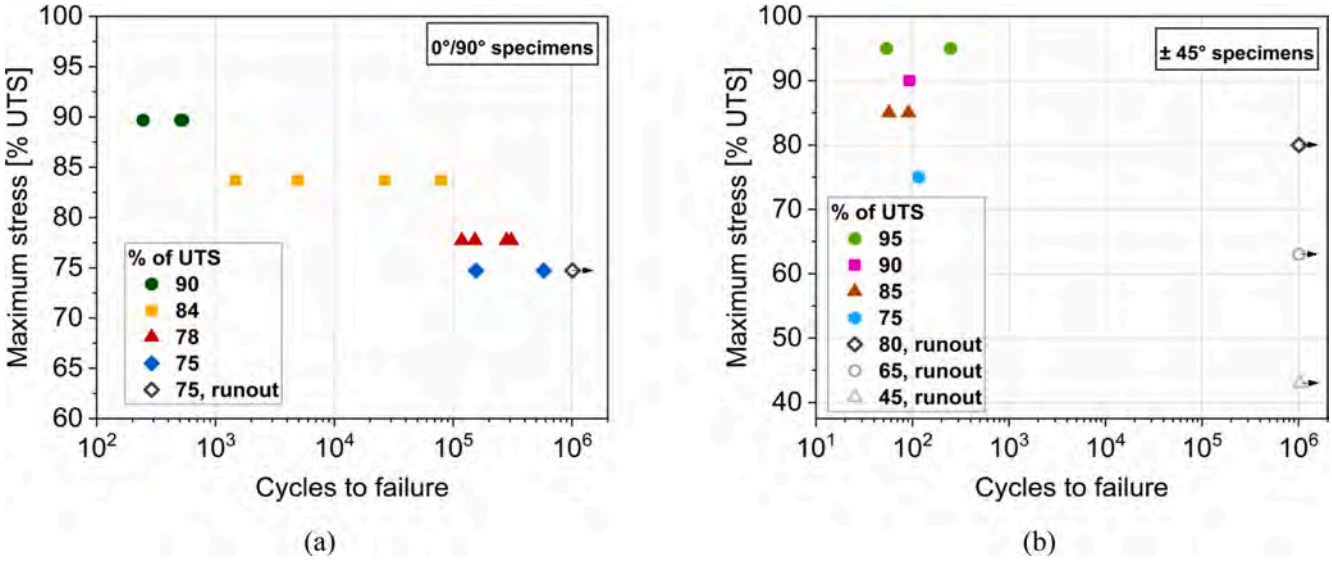

Fig. 6. Stress vs. number of cycles to failure for (a) 0°/90° and (b) ±45° specimens. Arrows indicate runouts.

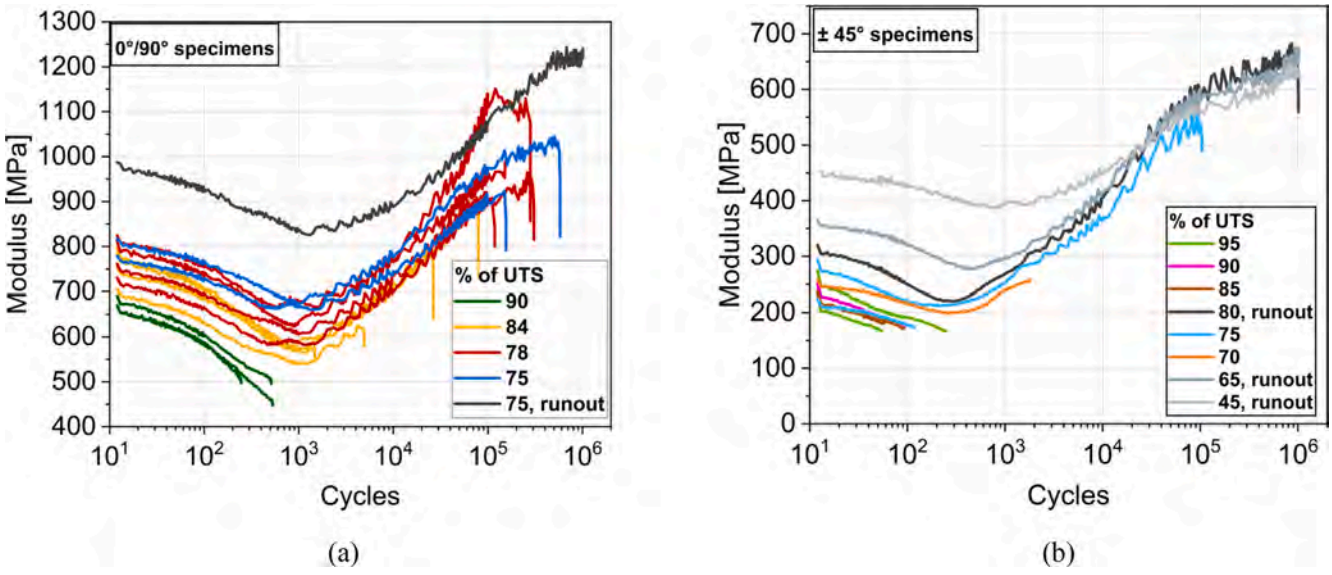

Fig. 7. Evolution of the dynamic modulus during fatigue of (a) 0°/90° and (b) ±45° specimens.

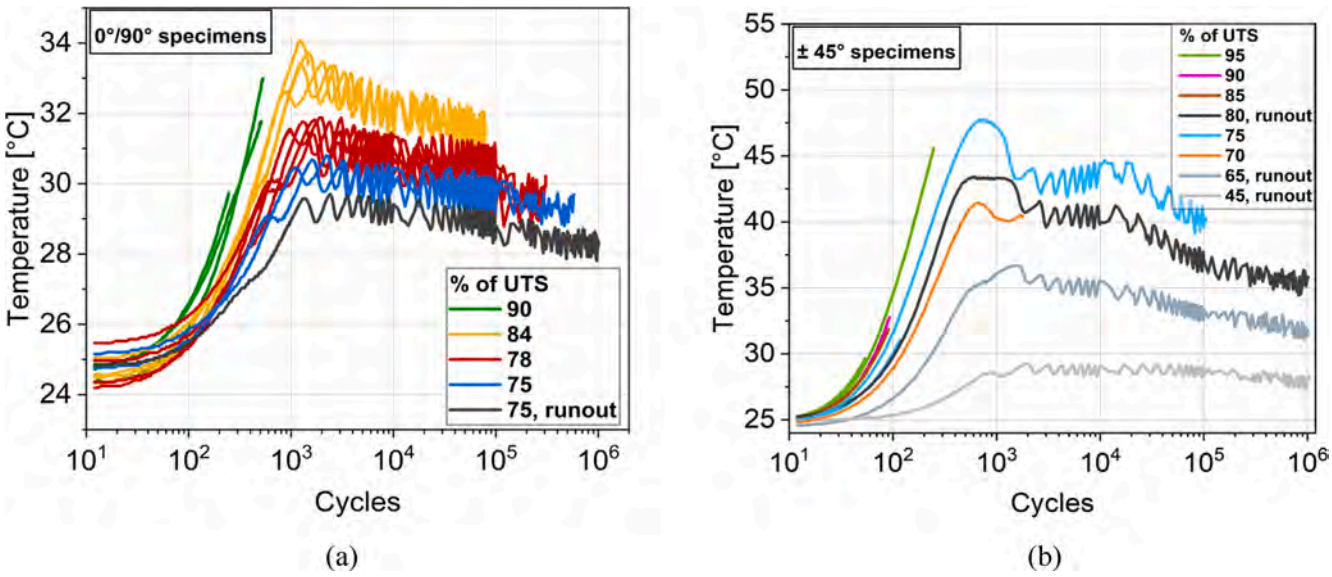

Fig. 8. Evolution of surface temperature of (a) 0°/90° and (b) ±45° specimens.

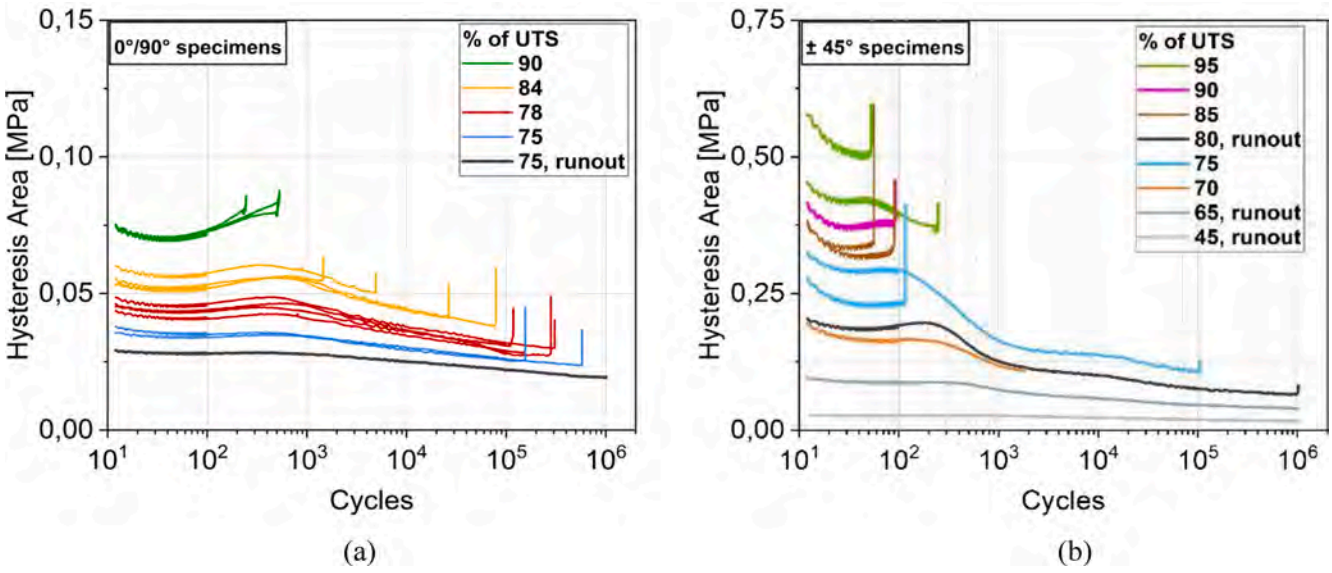

Fig. 9. Evolution of the hysteresis loop area during fatigue of (a) 0°/90° and (b) ±45° specimens.

Higher peak strains were recorded for higher applied loads, as expected (Fig. 10). Interestingly, most of the deformation occurred within the first few hundred cycles. Afterwards, provided failure did not occur, the peak strain of 0°/90° specimens increased much more slowly (Fig. 10a), while that of ±45° specimens remained virtually constant (Fig. 10b). ±45° specimens also experienced strains up to 10 times higher than 0°/90° specimens (Fig. 10a and 10b).

4. Discussion

4.1. Fatigue regimes

From the results, it is clear that two distinct fatigue regimes are present, one for higher and one for lower applied loads. These two regimes are known as thermal fatigue and mechanical fatigue respectively, as observed in both neat polymers [12,14–18] and SFRPs [21,24], and they differ greatly not only in the fatigue life, but also in the mechanical behaviour throughout fatigue. The thermal fatigue regime is characterized by a continuous increase in temperature until failure, while in the mechanical fatigue regime a stabilization temperature is reached. Specimens fatigued under higher (greater than 85% UTS) applied loads failed in the thermal regime, and showed a continuous softening up until failure (which occurred within a few hundred cycles). Specimens tested under lower applied loads (<85% UTS) failed in the mechanical fatigue regime. During the mechanical fatigue regime, which takes place once the specimen's temperature has stabilized, it can be observed that a strengthening mechanism takes place, in which as fatigue progresses, the material becomes stiffer and more 'elastic' (i.e., less viscous).

When testing at intermediate loads, the behaviour may be influenced by either regime: for 0°/90° specimens, this explains the huge scatter of results at the 84% load level. Thermal fatigue had more influence on specimens which failed earlier, and vice versa. Similarly, ±45° specimens at intermediate loads either failed very quickly thermally, or had a long life mechanically.

It can be observed from Fig. 8 that the temperature reached by

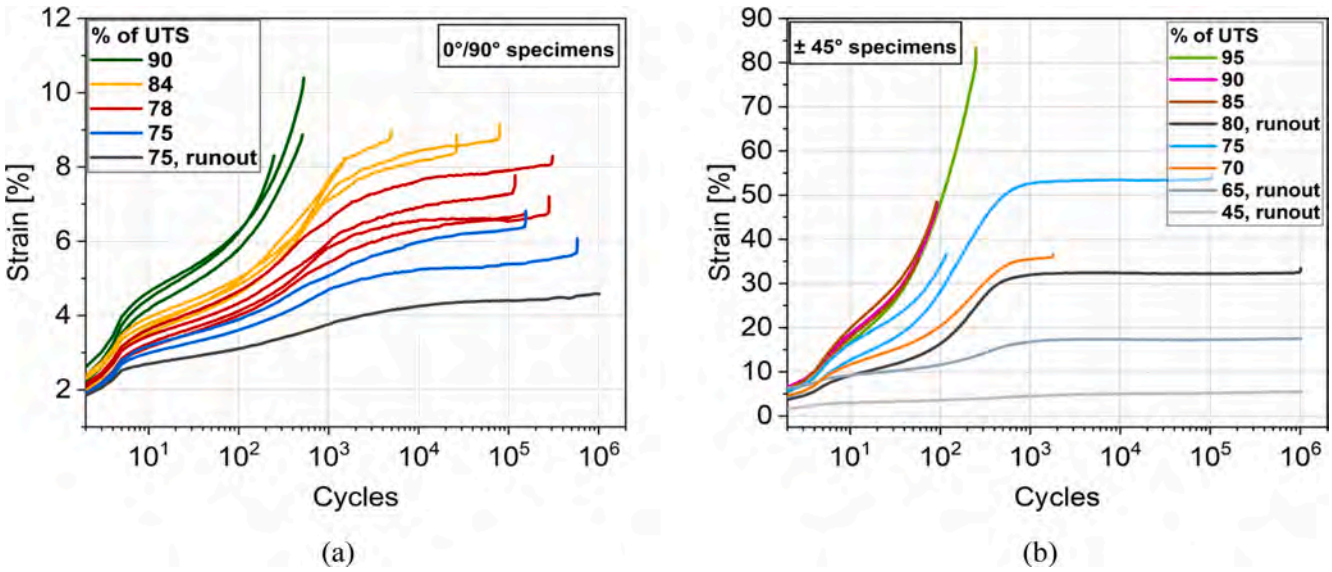

Fig. 10. Evolution of the peak strain in each cycle for (a) 0°/90° and (b) ±45° specimens.

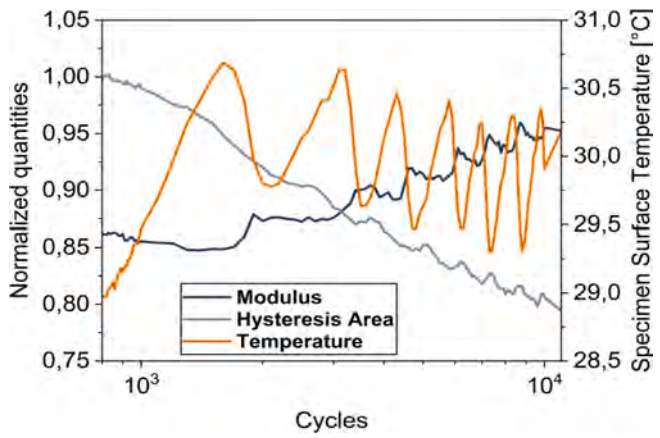

Fig. 11. Trends of the modulus, hysteresis area, and surface temperature for one specimen (84% Load, failed at 79,245 cycles).

specimens which failed in the thermal regime was not the highest of all tests. Previous work highlighted that deformation under fatigue loading is not uniform throughout the specimen [33]. Temperature is likely to present similar variations throughout the specimens, so it is possible that higher temperatures were reached at the failure location. The resistance thermometer measured the average specimen temperature on a wide area, so no conclusions can be drawn based on the absolute values of temperature at failure. Indeed, there are examples in literature in which thermally fatigued specimens failed at temperatures lower than those reached by mechanically fatigued specimens [21].

In Fig. 12 are illustrated the behaviours of thermally and mechanically fatigued 0°/90° and ±45° specimens, highlighting the different phenomena taking place during a fatigue test, which are summarized below:

- **Heating up (1):** At the start of the test, hysteretic heating causes the temperature in the specimen to increase. Due to this increase in temperature, the polyamide matrix of Onyx softens. The modulus decreases and the hysteresis area increases, which in turn causes more heat to be generated in each cycle.
- **Decrease in dissipation (2):** As a result of the cyclic load, changes take place in the material. This effect is initially hidden by the fast increase in temperature (which has a softening effect), but eventually the hysteresis area starts to decrease. This decrease is the first deviation from the initial trend: when it happens, the temperature is still rising, and the modulus is still decreasing.

For specimens failed in the thermal fatigue regime, only these first two phases take place (see Fig. 12.a and Fig. 12.c). Thermal effects due to hysteretic heating dominate the fatigue behaviours at high loads: the combination of the thermal softening and the high stresses involved leads to very rapid failure.

- **Stiffening (3) and cooling (4):** In mechanically fatigued specimens (see Fig. 12.b and Fig. 12.d) the heat generated in each cycle by self-heating is eventually balanced out by dissipation to the environment, and a maximum temperature is reached. Once the temperature stabilises, the modulus starts to increase. This increase is significant: the modulus eventually reaches values higher than the initial one. Meanwhile, since the hysteresis area is decreasing, less heat is being generated in each cycle, so a slight, but noticeable decrease in temperature is registered over time.

Both the stiffness and the hysteresis area are sensitive to temperature changes. This is not wholly unexpected, considering that the glass transition temperature of Onyx conditioned at 50% RH – 27 °C - is very close to room temperature [8].

The modulus's temperature sensitivity explains the softening displayed during the heating up period. The same behaviour was observed for neat injection moulded PA conditioned at 50% RH [14,20], while for dry as moulded PA (i.e. not close to its glass transition temperature [13]), virtually no softening was observed in mechanical fatigue [20]. Afterwards, temperature decreases by a few degrees. The observed increase in modulus is however too high than what justified by the cooling alone: even though the specimen's temperature remains quite high, the modulus reaches values even higher than the initial ones.

This stiffening mechanism was not observed in SFRPs or in FFF printed polymers. Most polymers, including polyamide [14,20], get stiffer under mechanical fatigue, but both injection moulded SFRPs and FFF printed neat polymers usually show a decrease in modulus as fatigue progresses [22,25,26,28,29]. A decrease in dissipation however has been observed for both [25,28], indicating that probably this mechanism is taking place, but its effect is hidden by other damage mechanisms, such as debonding between fibres and matrix (for the former) [23,24] and between beads (for the latter) [28]. The fact that Onyx

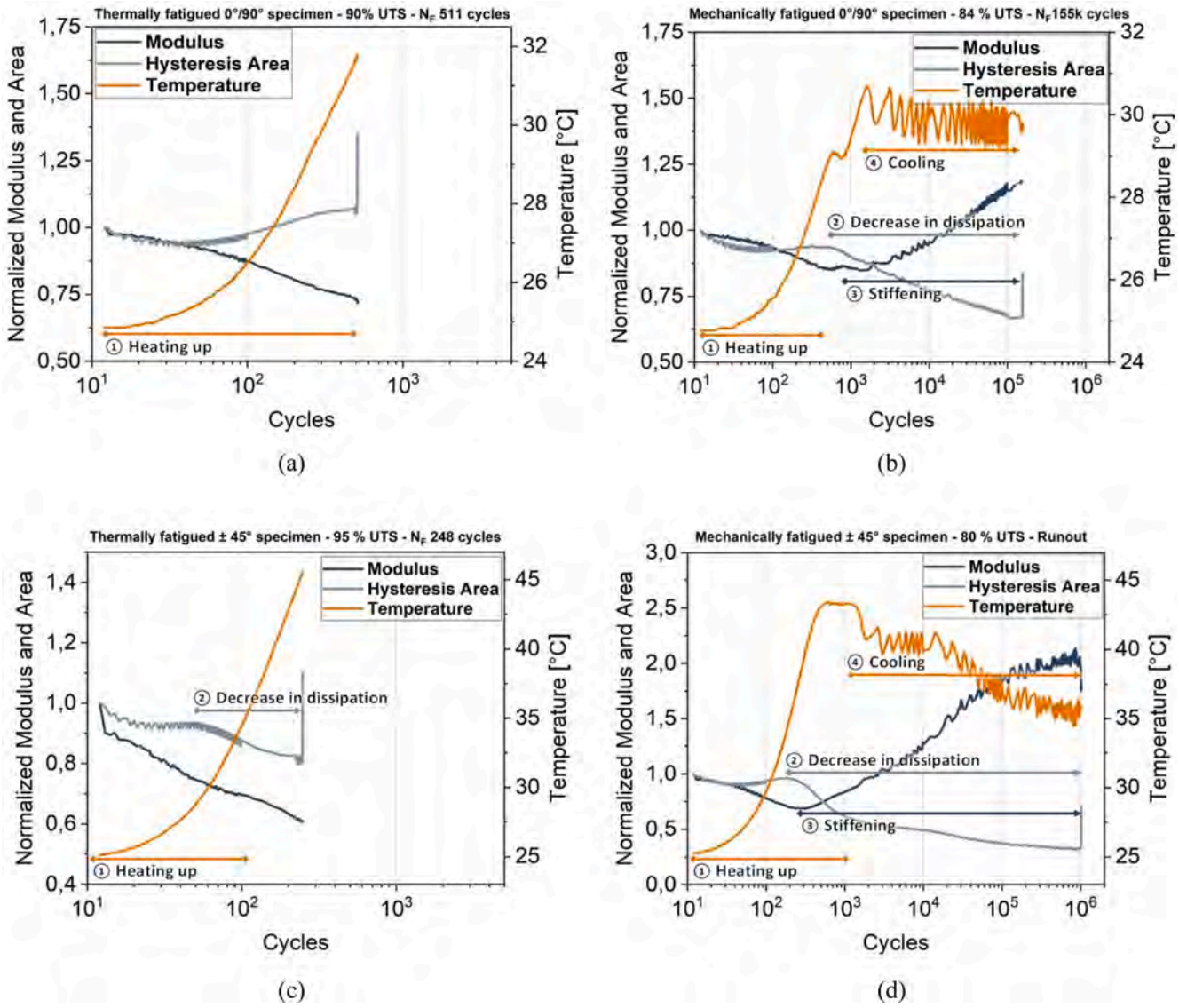

Fig. 12. Evolution of modulus, hysteresis area (both normalized to their initial value) and surface temperature for a (a) thermally fatigued 0°/90° specimen (90% load, 511 cycles to failure), (b) mechanically fatigued 0°/90° specimen (84% load, 155 k cycles to failure), (c) thermally fatigued ±45° specimen (95% load, 248 cycles to failure), and (d) mechanically fatigued ±45° specimen (80% load, runout).

shows such a significant degree of strengthening seems to indicate that the behaviour of the polymer matrix dominates over the other phenomena that may be taking place. This seems to indicate that, although the carbon fibre reinforcement in the filament does provide increased strength and stiffness [8], the Onyx fatigue behaviour is dominated by the polymeric matrix. This is most likely due to the low fibre content (16%), or to the very short fiber length (35 ± 5 μm) [8].

The reason for this strengthening likely lies in changes in the microstructure of the polymer, but its mechanism is not fully understood. The most common explanation is that, under tensile loading, polymeric chains progressively align with the load, increasing stiffness [16–18]. Other researchers attribute this behaviour to changes in crystallinity [14], to an acceleration of physical aging [34], or to the initiation and growth of crazes [35].

To investigate whether crystallinity did change as a result of fatigue, Differential Scanning Calorimetry (DSC) was performed on fatigued and unfatigued Onyx samples. Three were taken from a mechanically fatigued, and three from a thermally fatigued 0°/90° specimen, and their crystallinity was measured and then compared to one unfatigued sample. The results are shown in Fig. 13 and compared with results of a similar analysis for neat injection moulded polyamide done by Lesser et al. [14]. Onyx's crystallinity increased after fatigue cycling in both the thermal and the mechanical fatigue regime, with mechanical fatigue showing the highest increase. These results seem to indicate that microstructural changes are indeed taking place during fatigue. A higher crystallinity could justify the observed increase in stiffness. It is interesting to note how the thermally fatigued sample also shows an increase in crystallinity, suggesting that the same stiffening effect may have taken place, but its effects were hidden by thermal softening.

Injection moulded polyamide however shows a different behaviour: while crystallinity does increase after mechanical fatigue, it decreases after thermal fatigue. It's possible that this discrepancy could be due to the drastically different degree of crystallinity in the unfatigued samples, but further analysis is required to fully understand this effect.

4.2. *Effect of raster orientation*

The deformation mechanism of the ±45° specimens is different from that of the 0°/90° specimens, which has important effects on their mechanical behaviour. Under the applied load, the whole raster pattern

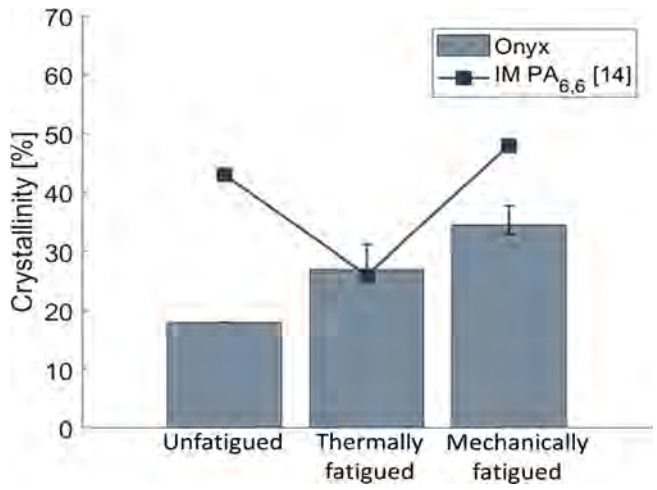

Fig. 13. Results of DSC analysis on virgin, thermally fatigued, and mechanically fatigued Onyx samples compared with injection moulded polyamide (from [14]).

deforms and rotates, so that the printed beads become more aligned to the loading direction. To highlight this phenomenon, individual beads were marked in white, and photographs were taken during the static tensile tests of ±45° specimens. By the end of the test, the raster angle increased from 45° to more than 60° (see Fig. 14).

A much higher elongation of the specimens is possible with limited strain on the individual beads [6]. Indeed, the strain at break, both in static and fatigue tests, was much higher for the ±45° specimens than for the 0°/90° ones.

While in the middle of the gauge length beads are free to rotate, inside the tabs their deformation is constrained (see Fig. 15.a). This causes high stress concentrations to arise near the tabs. This effect likely caused two of the ±45° specimens to fail near the tabs (Fig. 15.b). Such a failure cannot be considered for fatigue life assessments, since the stress state at the failure point is not as intended. To solve this issue, it's likely that an entirely different specimen geometry would need to be devised.

Since the raster angle changes during testing, it is expected that strength and stiffness increase, given the high anisotropy of this

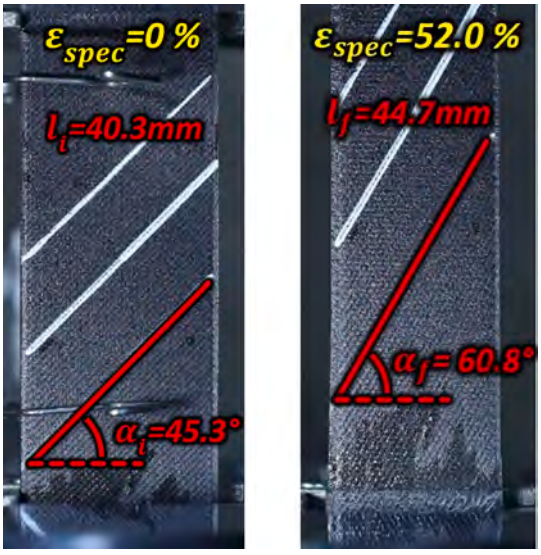

Fig. 14. Change in the raster angle of ± 45° specimens during tensile testing (from [6]).

material. This effect is not present for 0°/90° specimens, as their raster angle does not change during testing. Indeed, it can be seen in Fig. 7 and Fig. 12 that the relative increase in modulus is much higher for the ±45° raster orientation than for the 0°/90° one. It can also be noticed that, while for the 0°/90° specimens the minima in modulus and maxima in temperature happen at the same time, for the ±45° specimens the modulus actually increases after 200–1000 cycles, while the temperature decreases only after 1000–1500 cycles. The reason for this discrepancy is attributed to the change in raster angle happening during fatigue: most of the elongation experienced by the ±45° specimens occurs before 1000 cycles (see Fig. 10). When the modulus starts to rise, the temperature is still increasing. This softens the material, but this effect is likely hidden by the change in raster angle, which has the effect of increasing the stiffness.

Another important difference between the two raster orientations is in the degree of self-heating experienced during testing. For 0°/90° specimens, the temperature increase remained below 10 °C for all tests, while for 45° specimens it was more than twice as high, with temperatures reaching almost 50 °C. However, these higher temperatures are not wholly unexpected: given the much higher deformations, dissipative effects are also increased, leading to a higher degree of self-heating.

5. Conclusions

In this work, experimental tests were carried out to analyse the fatigue behaviour of an additively manufactured Short Fibre Reinforced Polymer. This material shows the presence of a thermally dominated and a mechanically dominated fatigue regime, either of which, depending on the applied fatigue load, may influence fatigue behaviour the most. Also, stiffening was observed to take place as a result of fatigue cycling. Both of these phenomena have not so far been documented in SFRPs produced by FFF.

In thermal fatigue (higher applied loads) hysteretic heating is the dominant effect. Specimens heat up rapidly and failure occurs quite fast. In the mechanical regime (lower applied loads) the temperature eventually stabilizes, and stiffening is observed. The material becomes more elastic, less viscoelastic, indicated by a decrease in dissipation. The dynamic modulus also increases significantly, after an initial softening period attributed to the initial heating of the specimen.

This strengthening behaviour during fatigue has been extensively documented for a number of injection moulded polymers, but for both short fibre injection moulded polymers and FFF-printed neat polymers the available literature showed only a decrease in modulus, although a decrease in dissipation was recorded for both.

Changes in crystallinity were recorded after fatigue cycling, which may be an indication of the underlying mechanism behind strengthening, but further work is required to confirm this hypothesis.

The printing layout has significant effects on the mechanical properties and fatigue behaviour. In this work, tests showed that specimens with a ±45° raster orientation displayed a lower modulus and much higher elongation at break. This elongation causes a change in raster orientation, which affects mechanical behaviour. Strains exceeding 50% were measured in fatigue, and self-heating phenomena were much more severe for ±45° specimens than for 0°-90° ones.

Fatigue testing of ±45° specimens presents some critical issues: the severe degree of deformation that they experience can create high stress concentrations close to the grips, which may lead to failure. Different specimen geometries should be investigated if further testing is to be done. Also, self-heating effects are very significant, even at low frequencies.

In conclusion, fatigue of FFF-printed SFRPs is a very complex phenomenon. It involves a variety of different mechanisms happening simultaneously, and is highly influenced by the properties and the behaviour of the polymeric matrix, as well as the raster orientation. Thermal effects, either from self-heating or from the environment, have an especially significant influence, and should not be neglected in

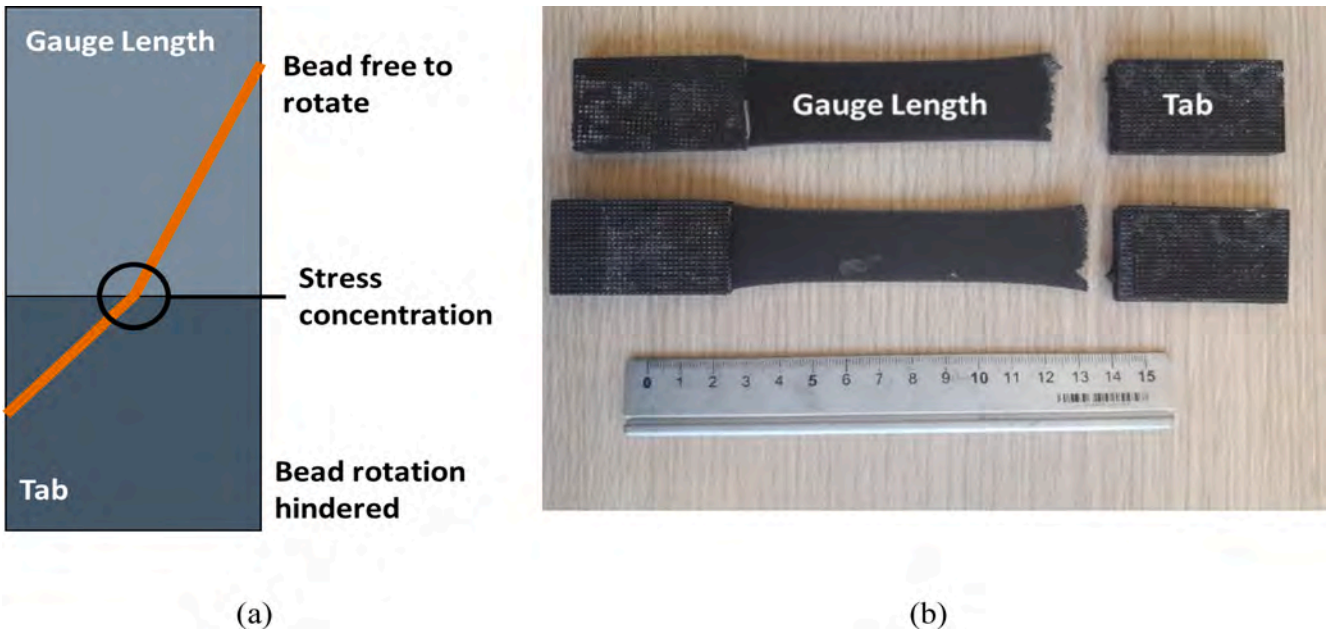

Fig. 15. Tab Failure in ± 45° specimens: (a) how a stress concentration arises near the tab, (b) the two specimens that experienced tab failure.

fatigue modelling of this material. While 3D printed composites do show a lot of potential, it's evident from the results of this work their fatigue behaviour requires further investigation to fully comprehend the peculiar aspects that have been highlighted in the present paper.

CRediT authorship contribution statement

A. Panerai: Methodology, Formal analysis, Investigation, Data curation, Writing – original draft, Visualization. **A. Canegrati:** Methodology, Investigation, Data curation, Writing – review & editing, Supervision. **L.M. Martulli:** Conceptualization, Methodology, Investigation, Resources, Writing – review & editing, Supervision. **M. Kostovic:** Resources, Investigation, Writing – review & editing, Supervision. **G. Rollo:** Resources, Investigation, Writing – review & editing, Supervision. **A. Sorrentino:** Resources, Writing – review & editing, Supervision, Project administration, Funding acquisition. **M. Carboni:** Conceptualization, Methodology, Investigation, Resources, Writing – review & editing, Supervision, Project administration, Funding acquisition. **A. Bernasconi:** Conceptualization, Methodology, Investigation, Resources, Writing – review & editing, Supervision, Project administration, Funding acquisition.

Declaration of Competing Interest

The authors declare that they have no known competing financial interests or personal relationships that could have appeared to influence the work reported in this paper.

Data availability

The data that has been used is confidential.

References

[1] Parandoush P, Lin D. A review on additive manufacturing of polymer-fiber composites. Compos Struct 2017;182:36–53. https://doi.org/https://doi.org/10.1016/j.compstruct.2017.08.088.
[2] Sun Q, Rizvi GM, Bellehumeur CT, Gu P. Effect of processing conditions on the bonding quality of FDM polymer filaments n.d.
[3] Pertuz AD, Diaz-Cardona S, González-Estrada OA. Static and fatigue behaviour of continuous fibre reinforced thermoplastic composites manufactured by fused deposition modelling technique. Int J Fatigue 2020;130:105275.
[4] Shanmugam V, Das O, Babu K, Marimuthu U, Veerasimman A, Johnson DJ, et al. Fatigue behaviour of FDM-3D printed polymers, polymeric composites and architected cellular materials. Int J Fatigue 2021;143:106007. https://doi.org/10.1016/J.IJFATIGUE.2020.106007.
[5] Afrose MF, Masood SH, Iovenitti P, Nikzad M, Sbarski I. Effects of part build orientations on fatigue behaviour of FDM-processed PLA material. Progress in Additive Manufacturing 2016;1:21–8. https://doi.org/10.1007/S40964-015-0002-3.
[6] Canegrati A, Martulli LM, Kostovic M, Rollo G, Sorrentino A, Carboni M, et al. Hygroscopic tensile and compressive behaviour of 3D printed short carbon fibre reinforced polyamide. Submitted to: Journal of Reinforced Plastics and Composites 2023.
[7] Lewicki JP, Rodriguez JN, Zhu C, Worsley MA, Wu AS, Kanarska Y, et al. 3D-printing of Meso-structurally ordered carbon fiber/polymer composites with unprecedented orthotropic physical properties. Sci Rep 2017:7.
[8] Pascual-González C, Iragi M, Fernández A, Fernández-Blázquez JP, Aretxabaleta L, Lopes CS. An approach to analyse the factors behind the micromechanical response of 3D-printed composites. Compos B Eng 2020;186:107820. https://doi.org/https://doi.org/10.1016/j.compositesb.2020.107820.
[9] Ding Q, Li X, Zhang D, Zhao G, Sun Z. Anisotropy of poly(lactic acid)/carbon fiber composites prepared by fused deposition modeling. J Appl Polym Sci 2020;137:48786.
[10] Liao G, Li Z, Cheng Y, Xu D, Zhu D, Jiang S, et al. Properties of oriented carbon fiber/polyamide 12 composite parts fabricated by fused deposition modeling. Mater Des 2018;139:283–92.
[11] Tekinalp HL, Kunc V, Velez-Garcia GM, Duty CE, Love LJ, Naskar AK, et al. Highly oriented carbon fiber–polymer composites via additive manufacturing. Compos Sci Technol 2014;105:144–50. https://doi.org/https://doi.org/10.1016/j.compscitech.2014.10.009.
[12] Janssen RPM, Govaert LE, Meijer HEH. An Analytical Method To Predict Fatigue Life of Thermoplastics in Uniaxial Loading: Sensitivity to Wave Type. Frequency, and Stress Amplitude 2005. https://doi.org/10.1021/ma071274a.
[13] Barbouchi S, Bellenger V, Tcharkhtchi A, Castaing P, Jollivet T. Effect of water on the fatigue behaviour of a pa66/glass fibers composite material. Journal of Materials Science - J MATER SCI 2007;42:2181–8. https://doi.org/10.1007/s10853-006-1011-x.
[14] Lesser AJ. Changes in mechanical behavior during fatigue of semicrystalline thermoplastics. J Appl Polym Sci 1995;58:869–79. https://doi.org/10.1002/app.1995.070580504.
[15] Launay A, Marco Y, Maitournam MH, Raoult I. Modelling the influence of temperature and relative humidity on the time-dependent mechanical behaviour of a short glass fibre reinforced polyamide. Mech Mater 2013;56:1–10. https://doi.org/10.1016/J.MECHMAT.2012.08.008.
[16] Kaiya N, Takahara A, Kajiyama T. Fatigue Fracture Behavior of Solid-State Extruded High-Density Polyethylene. Polymer Journal 1989 21:7 1989;21:523–31. https://doi.org/10.1295/polymj.21.523.
[17] Berer M, Tscharnuter D, Pinter G. Dynamic mechanical response of polyetheretherketone (PEEK) exposed to cyclic loads in the high stress tensile regime. Int J Fatigue 2015;80:397–405. https://doi.org/10.1016/J.IJFATIGUE.2015.06.026.
[18] Heinlein GS, Timpe SJ. Development of elastic and plastic properties of polyoxymethylene during bending fatigue. J Appl Polym Sci 2014;131:9225–34. https://doi.org/10.1002/APP.40762.

[19] Jo N, Takahara A, Kajiyama T. Analysis of Fatigue Behavior of High-Density Polyethylene Based on Nonlinear Viscoelastic Measurement under Cyclic Fatigue. Polym J 1993;25:721–9.
[20] Benaarbia A, Chrysochoos A, Robert G. Influence of relative humidity and loading frequency on the PA6.6 cyclic thermomechanical behavior: Part I. mechanical and thermal aspects. Polym Test 2014;40:290–8. https://doi.org/10.1016/J.POLYMERTESTING.2014.09.019.
[21] Esmaeillou B, Fitoussi J, Meraghni F, Tcharkhtchi A. Micro-mechanisms of fatigue in short glass fiber reinforced polyamide 66: A multi-scale experimental analysis. 16th European Conference on Composite Materials, ECCM 2014 2014.
[22] De Monte M, Moosbrugger E, Quaresimin M. Influence of temperature and thickness on the off-axis behaviour of short glass fibre reinforced polyamide 6.6 – cyclic loading. Compos Part A Appl Sci Manuf 2010;41:1368–79. https://doi.org/10.1016/J.COMPOSITESA.2010.02.004.
[23] Hitchen SA, Ogin SL. Damage accumulation during the fatigue of an injection moulded glass/nylon composite. Compos Sci Technol 1993;47:83–9. https://doi.org/10.1016/0266-3538(93)90099-3.
[24] Horst JJ, Spoormaker JL. Fatigue fracture mechanisms and fractography of short-glassfibre-reinforced polyamide 6. Journal of Mate Rials Science 1997;32:3641–51.
[25] Noda K, Takahara A, Kajiyama T. Fatigue failure mechanisms of short glass-fiber reinforced nylon 66 based on nonlinear dynamic viscoelastic measurement. Polymer (Guildf) 2001;42:5803–11. https://doi.org/10.1016/S0032-3861(00)00897-1.
[26] Frascio M, Avalle M, Monti M. Fatigue strength of plastics components made in additive manufacturing: first experimental results. Procedia Struct Integrity 2018;12:32–43. https://doi.org/10.1016/J.PROSTR.2018.11.109.
[27] Ziemian S, Okwara M, Ziemian CW. Tensile and fatigue behavior of layered acrylonitrile butadiene styrene. Rapid Prototyp J 2015;21:270–8.
[28] Terekhina S, Tarasova T, Egorov S, Skornyakov I, Guillaumat L, Hattali ML. The effect of build orientation on both flexural quasi-static and fatigue behaviours of filament deposited PA6 polymer. Int J Fatigue 2020;140:105825.
[29] Ziemian CW, Ziemian RD, Haile KV. Characterization of stiffness degradation caused by fatigue damage of additive manufactured parts. Mater Des 2016;109:209–18.
[30] Onyx Material Datasheet 2022. https://www-objects.markforged.com/craft/materials/CompositesV5.2.pdf.
[31] MarkForged. EIGER V1.0.3 2020 USER MANUAL 2020.
[32] Canegrati A, Martulli LM, Bolzoni G, Kostovic M, Rollo G, Sorrentino A, et al. 3D Printed Short Carbon Fibres Reinforced Polyamide: Tensile and Compressive Characterization and Multiscale Failure Analysis. Proceedings of the 20th European Conference on Composite Materials-Volume 3, 2022, p. 791–8. https://doi.org/10.5075/epfl-298799_978-2-9701614-0-0.
[33] Martulli LM, Canegrati A, Panerai A, Kostovic M, Rollo G, Sorrentino A, et al. Fatigue Characterization and Monitoring in 3D printed short fibres reinforced Polyamide. Composites Meet Sustainability – Proceedings of the 20th European Conference on Composite Materials, ECCM20, Lausanne, Switzerland: 2022.
[34] Liu LB, Yee AF, Lewis JC, Gidley DW. Structural changes in glassy polycarbonate induced by cyclic stresses. J Non Cryst Solids 1991;131–133:492–6. https://doi.org/10.1016/0022-3093(91)90346-8.
[35] Lesser AJ. Effective volume changes during fatigue and fracture of polyacetal. Polym Eng Sci 1996;36:2366–74. https://doi.org/10.1002/PEN.10634.